

# Neural Networks Approach for Predicting Slope Failure Areas Based on the Onsite Slope Survey Parameters at a Specified Mountain Road

**Tienfuan Kerh\***

Department of Civil engineering  
National Pingtung University of Science and Technology  
Pingtung 91027, Taiwan, \*email id: tferh@mail.npust.edu.tw

**Chih-Hung Tsenz**

Department of Civil engineering  
National Pingtung University of Science and Technology  
Pingtung 91027, Taiwan, email id: t88km@hotmail.com

\*Corresponding author

Date of publication (dd/mm/yyyy): 15/06/2018

**Abstract** – This study proposed a new method of using a neural network model for predicting slope failure areas by training different slope parameters obtained from 49 onsite slope failure surveys in a specified mountain road section. The developed model has three input parameters including slope height, slope horizontal distance, and rainfall factor. With three neurons in the hidden layer, a relatively better performance for predicting a slope failure area can be obtained in the output layer, based on the evaluation indices of a correlation coefficient and a mean square error. For all the data sets in the neural network calculation process, the square value of a correlation coefficient between the prediction result and the survey data reached up to 0.8020, which may imply that the developed model has an acceptable reliability. The current study has presented a simple way for dealing with this type of slope failure problem, and the obtained results may provide useful information for the relevant engineering agency to improve road safety in the mountain road region investigated.

**Keywords** – Neural Network Model, Evaluation Index, Slope Parameter, Rainfall Factor

## I. INTRODUCTION

Located in a subtropical region, the island of Taiwan is comprised of two-thirds mountain areas, suffers from heavy rains during the typhoon season every year, and that often causes mudslides with various slope failure problems on mountain roads. For instance, in 2009, the island was engulfed by Typhoon Morakot, which brought a continuously strong downpour, and the accumulated two-day duration of precipitation quantity was almost equivalent to the average annual rainfall in many regions (e.g. [1-2]). Without a doubt, this natural disaster event resulted in not only tremendous damage on the road system, but also caused a lot of casualties and economic losses. In order to improve the level of road safety for preventing further unexpected damages, it is crucial to analyze the slope failure problem either from an academic aspect or from a practical standpoint.

There is a wide range of researches in dealing with slope failure problems, such as to access the mechanism of slope failure behaviors and failure models in earlier years [3-4], and to classify the types of landslide depending on the specified local research areas [5-6]. For understanding the insights of slope failure more in detail, the theory of soil mechanics with the use of different numerical approaches under various geotechnical conditions are examined and

can be found in many previous literatures [7-13]. No matter which type of slope failure, the onsite situation probably becomes worse over time and may seriously endanger road users, so that the relevant engineering actions must be taken for maintaining the standards of road safety.

More importantly, for increasing slope stability, the topics of studying potential impact factors, and the reasons that cause slope failure, have attracted many researchers worldwide. For example, the factors that influence slope stability; in general, may include gravity, water, and unstable earth materials, as that various slope failure events have been reported in many countries [14]. For a more specific topography and weather conditions comparable to the Taiwan area, the external induced reasons of a landslide may include rivers, road distance, rainfall, land use, and sand sediment. Whereas, the potential factors to bring about slope failure may include a falling gradient, geological condition, slope direction, elevation, and vegetation [15]. The above-mentioned factors can be used for planning potential slope failure, which may provide a good index for land management, and for setting up a warning system in the studied area.

Following the progress of information technology, the recently developed computational intelligence also plays an important role for evaluating various slope failure problems [16-21]. These studies may open a track for analyzing slope failure related problems by using the most popular neural network approach. However, among those studies, including all of the above-cited references it is hard to find an investigation for modeling the total area of slope failure with the potential impact factors at a specified road section. As this is one of the useful research topics for predicting the scale of slope failure, and for evaluating the potential at other locations. Therefore, the objective of this study is to perform an onsite survey for collecting data including the total area of slope failure, slope horizontal length, slope height, slope angle, and rainfall from nearby checking stations, along a mountain road section in Pingtung county, Taiwan. Based on the actual 49 measured data sets, the neural network method is adopted for linking these different parameters, and an estimation model is developed for predicting the total area of possible slope failure at unmeasured sites. The proposed method may provide relevant engineering agencies with a useful approach to estimate a slope failure area, and may provide help for straightening and/or renovating the

mountain road slopes.

## II. RESEARCH AREA AND ONSITE INVESTIGATION DATA

### A. Geological and Hydrological Conditions

Displayed in Fig. 1 is the map information and sketch of the research area in this study. There are a total of 49 measurement locations, three rain checking stations, and three extra slope failure locations in the neighborhood of the chosen mountain road sections. The research area in basic belongs to the southern part of Taiwan's central

mountain ridge, which is primarily composed of hard shale or slate. The distribution of geological conditions in this area mainly includes alluvium, terraces stacked layers, and sedimentary rocks. The deposit environment presents an unstable phenomenon, which may present a sedimentary slump structure and a sliding surface. Further, the mountain saddle is about 30-45 degrees in a northern direction and inclined to the eastern side, which has a potential failure resulting from the slope of the easy flow direction [22]. Thus, slope failure could happen due to poor geological features and a long-term action of weathering and corrosion on central mountain slate block.

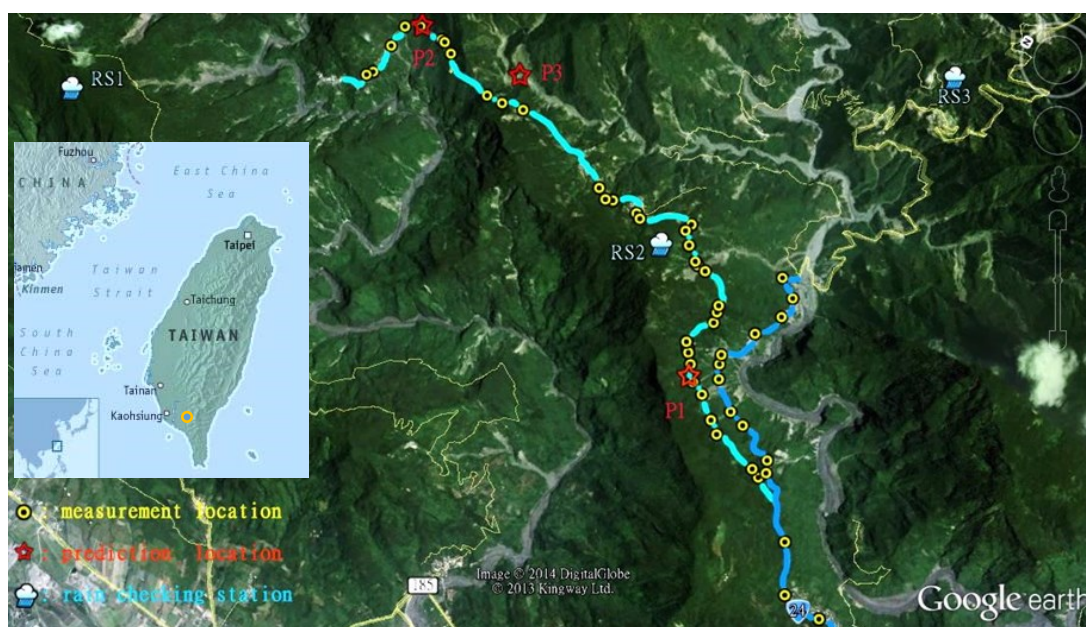


Fig. 1. Research location and blow up of the mountain road section (map sources: google and <http://www.taiwandc.org/economist-2005-01.htm>)

The present research area is situated at the neighbourhood of the Kaoping River watershed, which is the largest river basin in Taiwan that belongs to a tropical weather zone, which has a distinct dry and wet season. The distribution of precipitation in this river basin is quite uneven over an entire year. The average annual rainfall is 2522 mm, where about 90% is concentrated from May to October, due to the southwest monsoon and the onset of typhoons [23]. As the geological condition presents a

tattered structure, the ground water is hard to maintain constantly in this research mountain road section, but it still has some seepage within the water bearing bed. With the above brief descriptions of the geological and hydrological conditions, and as seen in Fig. 2, is an example of slope failure at one of the research measurement locations. From the satellite map and onsite picture, it can be found that the slope has been damaged quite seriously, and that may endanger road users.



Fig. 2. An example of slope failure based on satellite map and onsite observation.

### B. Onsite Investigation Data

For a more specific description, the present investigated area, starting from highway Tai24 transfer, to the county road of Ping31, to the villages of Derwin and Darser, as well as from 26.8k of highway Tai24, to the Guchun Bridge. The tools needed for an onsite survey in this study including: (1) A Nikon forestry pro 550 laser telescope, which can be used for measuring and calculating slope angle, slope height, and slope width. (2) A global positioning satellite (GPS) alignment gauge for recording coordinates of the slope. (3) A digital camera for taking pictures of the onsite slope landscape; and (4) a tape measure for checking the slope length.

Shown in Table 1 is some of the data set calculated and

revised in accordance with the measuring standpoint for the 49 slope failure places as found on the mountain roads by the onsite investigation. From the total of actual slope failure cases, we can find that there are around 71% have a slope height of less than 30m; there is more than a half (52%) that has a slope angle between 30° to 45°, and for the cases of slope angel over 45°, that also occupies a larger percentage (45%). From the investigation of slope failure areas, we can find that there are 45% of the total cases those have an area of less than 1000m<sup>2</sup>; and there are 43% those have an area between 1000m<sup>2</sup> to 10000m<sup>2</sup>. These slope failure related data sets will be used with the following rainfall data for developing a prediction model from a neural network approach.

Table 1. Slope failure data set in the investigated mountain road sections.

Highway Ping31	Coordinates		Slope height (m)	Slope angle (°)	Slope hypotenuse (m)	Horizontal length (m)	Failure area (m <sup>2</sup> )
	N	E					
1	22°48'28.22"	120°41'57.29"	7.00	78.86	7.13	1.38	178.25
2	22°48'26.36"	120°42'00.21"	26.40	33.56	47.76	39.80	2378.45
3	22°48'24.87"	120°42'15.21"	9.40	44.34	13.45	9.62	653.67
4	22°48'23.39"	120°42'26.14"	20.00	41.30	22.77	22.77	4999.50
5	22°48'17.05"	120°42'29.69"	14.00	61.30	15.96	7.66	379.80
6	22°48'05.38"	120°42'28.64"	11.00	51.50	14.06	8.75	444.30
7	22°47'58.65"	120°42'24.92"	128.00	29.02	263.86	230.73	16623.18
8	22°47'35.04"	120°42'12.48"	33.80	43.32	49.27	35.85	6405.10
9	22°47'27.85"	120°42'16.43"	13.00	34.87	22.74	18.66	500.28
10	22°47'18.43"	120°42'18.66"	71.00	49.33	93.61	61.00	40626.74
...	...	...	...	...	...	...	...
31	22°45'50.43"	120°42'06.10"	12.00	35.09	20.87	17.08	500.88
32	22°45'40.12"	120°41'55.99"	13.00	41.98	19.44	14.45	651.24
33	22°45'34.36"	120°41'54.50"	12.40	32.65	22.99	19.35	966.00
34	22°45'26.02"	120°41'21.71"	11.60	37.95	18.86	14.88	1131.60
35	22°45'24.00"	120°41'19.37"	14.80	49.17	19.56	12.79	469.40
Highway Tai24	Coordinates		Slope height (m)	Slope angle (°)	Slope hypotenuse (m)	Horizontal length (m)	Failure area (m <sup>2</sup> )
	N	E					
36	22°43'37.63"	120°40'01.57"	18.00	45.45	25.26	17.72	540
37	22°43'55.09"	120°40'03.25"	30	33.01	55.07	46.19	4536
38	22°44'06.32"	120°40'24.42"	14.8	40.43	22.82	17.37	621
39	22°44'27.66"	120°40'47.75"	46.6	37.28	76.93	61.21	10815.75
40	22°44'29.62"	120°40'53.25"	27.4	32.32	51.25	43.31	6720
...	...	...	...	...	...	...	...
47	22°45'01.42"	120°42'15.04"	24.4	47.77	32.95	22.15	1761.75
48	22°44'53.54"	120°41'04.62"	57	48.35	76.28	50.70	7315
49	22°44'46.11"	120°41'01.79"	9.2	54.92	11.24	6.46	779

Many factors may affect the occurrence of slope failure, where the rainfall distribution in the investigation area is one of the primary reasons for causing slope instability. Therefore, this study has collected rainfall data from the three rainfall checking stations in the neighborhood of the research area to take into account this important factor in the model analysis. As collected from the Central Weather Bureau of Taiwan, and displayed in Table 2, is the monthly rainfall recorded data set for a sequential four years. It can be found that the rainfall is, in general,

concentrated from April to October. By taking the average monthly rainfall during this period as a basis, and by using a weight-based method for calculating rainfall distribution in the investigation area, and from the spatial relationship between the places of slope failure and the rainfall checking stations. The obtained rainfall data for each place of the slope failure can then be used with the above mentioned slope failure data for developing a neural network prediction model.

Table 2. Monthly rainfall distribution from three nearby checking stations in the investigation area (source: Central Weather Bureau).

RS1 (Weilliao rain station)									unit: mm				
Y-M	1	2	3	4	5	6	7	8	9	10	11	12	Avg.(4-10)
2008	27.5	15.5	25.5	148.5	275	995	1879	240	1731.5	238	95.5	2	786.7
2009	0.5	9	76.6	281	114	724.5	256	3268.5	327	132.5	5.5	4.5	729.1
2010	13.5	50	11.5	84	764	629.5	615.5	359	1352	350	29.5	33.5	593.4
2011	37.5	9	20	67	447	237.5	296	8	220	282.5	164	42.5	222.6
RS2 (Shanderwin rain station)									unit: mm				
2008	20.5	23.5	25.5	173	437	892.5	1885	233.5	1554	174.5	48	0	764.2
2009	0	3	85.5	358.5	154	546	249.5	2357	117	66.5	2.5	3.5	548.8
2010	12.5	35.5	9.5	65	631.5	486.5	582.5	203.5	1234.5	277.5	28	27	497.3
2011	27.5	3	13	76	332.5	247.5	644.5	767	343.5	143	154	48	364.9
RS3 (Ali rain station)									unit: mm				
2008	21	19.5	32.5	223.5	430	906.5	1539	260	800	80	54.5	0	605.6
2009	0	5	76.5	119.5	51.5	483.5	266.5	1227	89.5	83.5	1.5	4.5	331.6
2010	13	30	9.5	63	476	434	450	158.5	665.5	284	26.5	19	361.6
2011	25.5	3	21.5	66.5	336	204.5	519	725	131.5	115	195	42.5	299.6

### III. NEURAL NETWORK APPROACH

#### A. Calculation Process of a Neural Network

In the community of computational intelligence, that includes several methods such as artificial neural network, evolutionary computation, and fuzzy logic, for solving various complicated and inverse problems. Among these methods, the back-propagation neural network is widely used for the prediction and pattern recognition, as per many related papers that have been published [24-28]. The main characteristic of the back-propagation neural network is the nonlinear transformation between the different layers, which possess a high learning ability for parameter prediction. The basic structure of this multi-layered neural network consists of an input layer, a hidden layer, and an output layer. The detailed algorithm of the back-propagation neural network model can be seen in relevant references (e.g. [29-31]). Briefly, the mathematical equation of this approach can be written as:

$$Y_j = F(net_j) = F(\sum W_{ij}X_i - \theta_j) \quad (1)$$

where  $Y_j$  is the output of neuron  $j$ ;  $W_{ij}$  is the weight from neuron  $i$  to neuron  $j$ ;  $X_i$  is the input signal generated for neuron  $i$ ; and  $\theta_j$  denotes the bias value associated with neuron  $j$ . The Sigmoid function is frequently used for the nonlinear activation function as it is easier to make the operating process continuous and differentiable.

In order to reduce the difference between the network outputs ( $T_k$ ), and the target values ( $Y_k$ ), an error function ( $E$ ) may be defined as the following equation to represent a measure of the neural network performance.

$$E = \frac{1}{2} \sum (T_k - Y_k)^2 \quad (2)$$

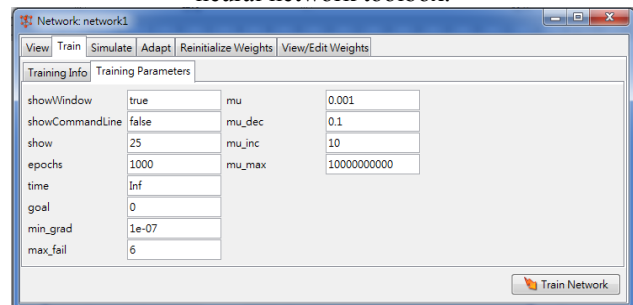
For minimizing the above error function, the steepest gradient descent method is often adopted to update the network weight and bias values in the direction in which

the performance function decreases most rapidly, and the negative of the gradient in the learning process. In the iterative procedure of the training neural network, the amount of weight update based on this gradient direction along with a step size may be written as:

$$\Delta W_{ij}(n) = -\eta \frac{\partial E(n)}{\partial W_{ij}(n)} + \alpha \Delta W_{ij}(n-1) \quad (3)$$

where  $\eta$  is the parameter of the learning rate, which can affect the speed of approach to the minimum solution. Additionally, the symbol  $\alpha$  is the momentum parameter, which can determine the amount of influence between two successive iterations, and can be used to prevent the system from converging to a local minimum.

Table 3. An example of training parameters in the neural network toolbox.



Parameter	Value
showWindow	true
showCommandLine	false
show	25
epochs	1000
time	Inf
goal	0
min_grad	1e-07
max_fail	6
mu	0.001
mu_dec	0.1
mu_inc	10
mu_max	10000000000

In this study, the software package MatLab is used in the calculation process, where the choice of  $\mu$  (mu) in the neural network toolbox can directly affect the error convergence [32]. Shown in Table 3 above is an example case of parameters set up in the neural network toolbox. The epochs represent training times; max\_fail is error tolerance; min\_grad is least relative error; mu is initial value; mu\_dec is decreasing coefficient; mu\_inc is increasing coefficient; and mu\_max is maximum value. These parameters with other choices, such as the learning rate, and the momentum factor based on the problem

studied, can be used to complete the calculation process in neural network training.

### B. Model Architecture and Evaluation Index

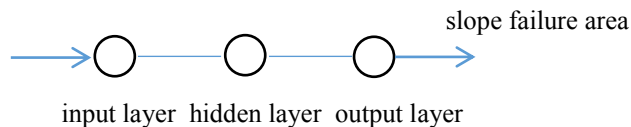
To develop an acceptable neural network model for prediction, the slope failure data set is initially normalized in the range of 0 to 1 for preventing the effect of extreme values. The data set is then randomly divided into three groups, where 70%, 20%, and 10% of the total data set are used for training, validation, and to test the model. From the slope failure data set, the parameters of the slope height, slope angle, slope hypotenuse, slope horizontal length, and rainfall, will be used in the input layer. Nonetheless, by considering the slope hypotenuse is post-calculated from the slope height and the slope horizontal length, therefore, this parameter will be skipped for facilitating the model's development. Although the parameter of the slope angle also relates to the slope height and the slope horizontal length, this directly measured parameter is still kept for investigation. With different neurons in the hidden layer, the slope failure area is taken in the output layer as the target value.

For checking the sensitivity of the slope parameters in the neural network model, as displayed in Fig. 3, the architecture of the three neural network models will be

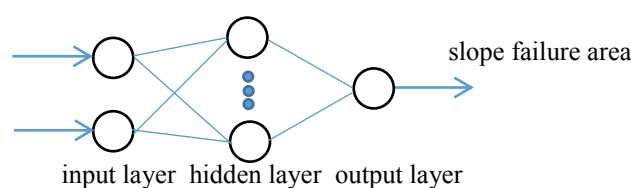
investigated in this study. Model1 has one input parameter which may include slope height ( $h$ ), or slope angle ( $a$ ), or slope horizontal length ( $l$ ), or rainfall ( $r$ ), independently (i.e.,  $I_h$ ,  $I_a$ ,  $I_l$ ,  $I_r$ ). One neuron in the hidden layer and the output is the slope failure area ( $A$ ). Model2 has two input parameters, from the combination of the above mentioned four parameters (i.e.,  $I_{ha}$ ,  $I_{hl}$ ,  $I_{hr}$ ,  $I_{al}$ ,  $I_{ar}$ ,  $I_{lr}$ ). The neurons can be varied from one to three in the hidden layer, and the output is also the slope failure area. Model3 has three input parameters, also from a combination of the four input slope failure related factors, but the rainfall factor must be kept in the combination (i.e.,  $I_{har}$ ,  $I_{hlr}$ ,  $I_{alr}$ ). The neurons can also be varied from one to three in the hidden layer, and the output is the same as the previous models.

The most commonly adopted indices to evaluate the performance of a neural network model are the coefficient of correlation ( $R$ ), and mean square error ( $mse$ ). Note that the definition of these two evaluation indices will not be shown here in this paper, as they can be easily found in previous literatures (e.g. [33-34]). With all the above methodology discussions, the performance and prediction result of a neural network approach in analyzing the slope failure problem can then be illustrated in the following section.

Model1



Model2



Model3

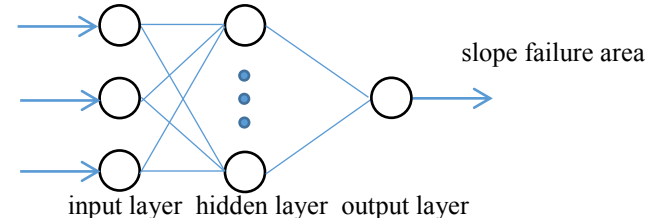


Fig. 3. Three neural network models with different neurons in the hidden layer.

## IV. NEURAL NETWORK MODEL PERFORMANCE AND PREDICTION RESULT

### A. Comparison of Model Performance

As mentioned in the previous section, there are four slope failure parameters; those can be used in the input layer to develop a neural network model for predicting a slope failure area in the output layer. In order to obtain a relatively better neural network model, it is a necessary requirement to check the performance of each model based on the input parameters. The number of neurons in the hidden layer may have an influence on the accuracy of prediction, and the neurons may be chosen in accordance with these two ways [35]. One is the so-called pruning algorithm; that is, a training algorithm that progressively reduces the number of neurons in the hidden layer, and training the neural network until a better model is found. On the other hand, the constructive algorithm is a training algorithm that successively adds neurons to the hidden layer in order to determine a better neural network model.

For simplification, this study uses the constructive algorithm that start from one neuron to three neurons in the hidden layer. As the input parameters are no larger than three neurons, so it believes that the chosen neurons in the hidden layer can sufficiently acquire an acceptable output result.

Based on the evaluation index of the correlation coefficient, as shown in Table 4, is the performance of the neural network models with various input slope failure parameters. From the results of Model1, we can find that the parameters of the slope angle and the rainfall factor are relatively insignificant, but the rainfall factor seems to have a better performance ( $R^2 = 0.1956$ ) than that of the slope angle ( $R^2 = 0.0612$ ). The combination of these two factors can also be found to have a relatively poor performance in Model2 ( $I_{ar}H_nO_A$ , average  $R^2 = 0.1698$ ), and that may imply that the parameter of the slope angle may be neglected. Moreover, from Model3, we can see that the model of  $I_{hlr}H_nO_A$  has the best performance with an average of  $R^2 = 0.6869$ . In particular, the combination

of using three input parameters (slope height, slope horizontal length, and rainfall factor), with three neurons in the hidden layer, can achieve the best performance ( $R^2 = 0.8020$ ) for the models studied herein.

Table 4. Comparison of model performances with different neurons in the hidden layer.

R <sup>2</sup> (all data)		Neurons in the hidden layer			R <sup>2</sup>
NN models		1	2	3	Average
Model1	I <sub>h</sub> H <sub>n</sub> O <sub>A</sub>	0.6068	-	-	0.6068
	I <sub>a</sub> H <sub>n</sub> O <sub>A</sub>	0.0612	-	-	0.0612
	I <sub>i</sub> H <sub>n</sub> O <sub>A</sub>	0.6042	-	-	0.6042
	I <sub>r</sub> H <sub>n</sub> O <sub>A</sub>	0.1956	-	-	0.1956
Model2	I <sub>ha</sub> H <sub>n</sub> O <sub>A</sub>	0.5469	0.5942	0.5849	0.5753
	I <sub>hl</sub> H <sub>n</sub> O <sub>A</sub>	0.6275	0.6352	0.6310	0.6312
	I <sub>hr</sub> H <sub>n</sub> O <sub>A</sub>	0.5802	0.5716	0.6098	0.5872
	I <sub>al</sub> H <sub>n</sub> O <sub>A</sub>	0.5725	0.5745	0.6037	0.5836
	I <sub>ar</sub> H <sub>n</sub> O <sub>A</sub>	0.1376	0.2120	0.1597	0.1698
	I <sub>r</sub> H <sub>n</sub> O <sub>A</sub>	0.5295	0.5764	0.6471	0.5843
Model3	I <sub>har</sub> H <sub>n</sub> O <sub>A</sub>	0.5866	0.5408	0.5885	0.5720
	I <sub>hrl</sub> H <sub>n</sub> O <sub>A</sub>	0.6275	0.6400	0.8020	0.6898
	I <sub>alr</sub> H <sub>n</sub> O <sub>A</sub>	0.5844	0.5955	0.6049	0.5949

Note that during the neural network training process, it is found that the use of the momentum term  $\alpha = 0.3$  or  $0.5$ , as well as the learning rate  $\eta = 0.3$  or  $0.5$ , has a reduced convergent rate. However, the use of  $\alpha = 0.9$  and  $\eta = 0.9$ , the mean square error can converge in a more stable manner and more quickly. Hence, these two parameters are employed for all of the trainings in the neural network models. As shown in Fig. 4, the example of convergent tendency for the best case I<sub>hrl</sub>H<sub>3</sub>O<sub>A</sub>, the least error (mse = 0.005343) occurs at epoch 16 during the total neural network calculation process. For this model, Fig. 5 is the distribution of the target value with the neural network output result, where the square value of the correlation coefficient are  $R^2 = 0.81467$ ,  $0.7086$ ,  $0.86532$ , and  $0.8020$ , for training, validation, test, and all data sets, respectively. Therefore, this preferred neural network model is believed to have a higher reliability and it will be taken for further prediction work.

### B. Prediction Result for Unchecked Site

The above analyzed results show that the development of the neural network model by adopting input parameters including slope height, slope horizontal length, and rainfall, can have an acceptable performance for predicting the slope failure area in the output. For the total 49 slope failure cases, as presented in Fig. 6, is the plot of the prediction results versus survey data. Because the data is randomly distributed, we can find that the neural network prediction results exhibit an irregular shape, but the tendency is, in general, reasonable in agreement with the slope failure survey data, particularly for the region of the slope failure area under  $20000\text{m}^2$ . To view the prediction tendency more clearly, as shown in Fig. 7, the rearranged plot result from a small value to a large value, and that a more significant agreement can be found between the prediction and survey data. Indeed, the discrepancy between prediction and onsite survey still exhibits relatively large from these plots. The results may be

improved by considering different approaches, but it is temporary out scope of this study.

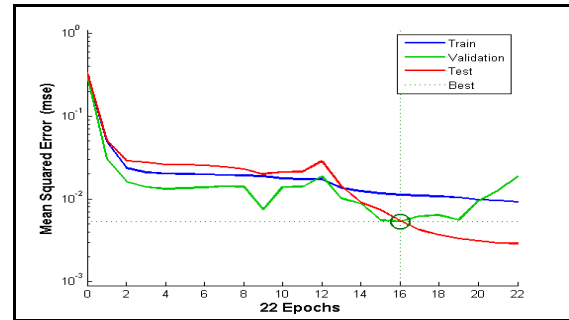


Fig. 4. Convergent tendency for the model I<sub>hrl</sub>H<sub>3</sub>O<sub>A</sub>.

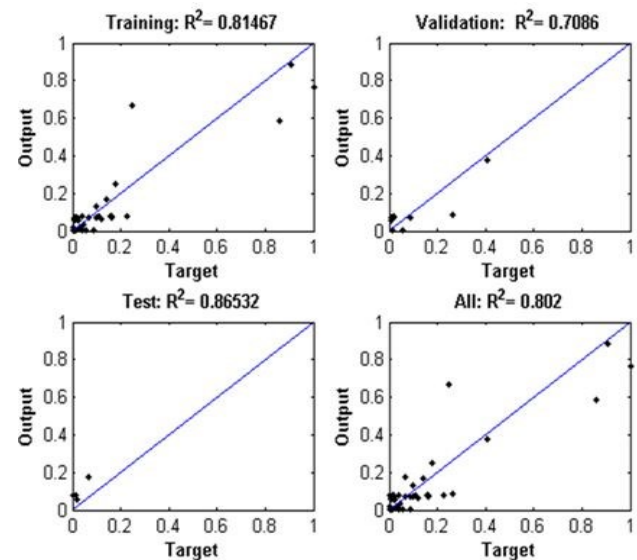


Fig. 5. Distribution of output with target value for the neural network model I<sub>hrl</sub>H<sub>3</sub>O<sub>A</sub>.

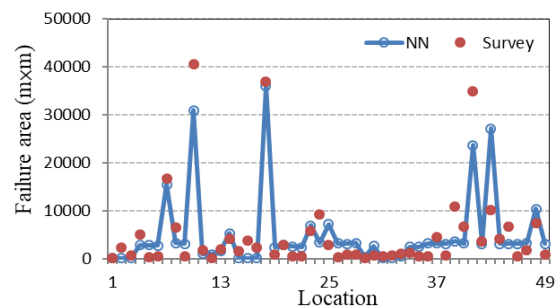


Fig. 6. Plot of prediction result with survey data.

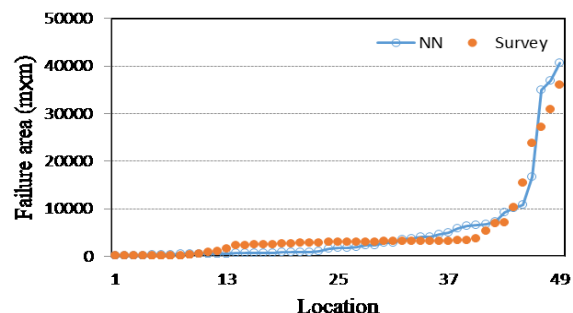


Fig. 7. Replot of prediction result with survey data.

In order to increase the applicability of the neural network model developed in this study, three newly found slope failure places (P1, P2, and P3, as seen in Fig. 1) in the neighborhood of the research region, due to the recently occurred typhoon events, are taken to test the model. As displayed in Fig. 8 is the comparison of the prediction result with the survey data, and we can find that the differences of the slope failure area are 0.001%, 42.0%, and 24.5%, for the three slopes P1, P2, and P3, respectively. The obtained result seems not to present a stable performance, one (P1) has a very good prediction result, but (P2) has a poor prediction result. This implies that the developed neural network may require an improvement for increasing the prediction accuracy.

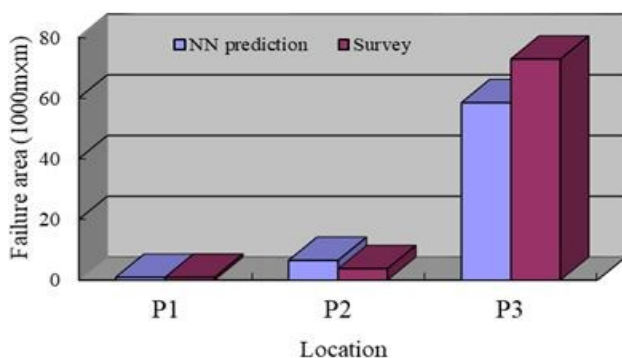


Fig. 8. Comparison of prediction result with survey data for three newly found slope failure places.

Note that the present study collected only 49 actual slope failure cases as the basis for training, verification, and testing the neural network model, the total data set may not be sufficient to develop a reliable prediction model. Also, we may expect to acquire a better result if some of the extreme data are skipped in the training process of the neural network model, but the drawback of this treatment may reduce the flexibility of the developed model. In addition, the reliability of the method proposed in this study may be improved by incorporating a genetic algorithm with a global searching capability in the neural network model, and that may be considered for future study and used for a wider range of applications. Nonetheless, the present study does provide a new and simple method for dealing with this type of slope failure problem, and the obtained results may well provide useful information for the specified mountain road sections.

## V. CONCLUSION

The slope failure problem is one of crucial research topics in the field of civil related engineering, particularly on a mountain road composed of slopes with various conditions. This study proposed a method of adopting a neural network model for predicting a slope failure area based on the different input slope parameters, including slope height, slope angle, slope horizontal distance, and rainfall factor, collected from 49 onsite slope failure surveys on the mountain roads of Taiwan. Although the principle of neural network model is not a new methodology, the application to link the above mentioned

parameters can consider as a novel approach to solve this type of slope failure problem.

From the evaluation indices of the correlation coefficient and the mean square error, the results showed that the parameter of a slope angle is relatively insignificant. The combination of using slope height, slope horizontal distance, and rainfall data in the input layer, with three neurons in the hidden layer, could achieve the best performance for predicting the slope failure area in the output layer. The squared values of the correlation coefficient were 0.8147, 0.7086, and 0.8653, for the three stages in the neural network calculations, i.e., training, validation, and test, respectively. For all the data sets, the index value reached 0.8020, and thus the developed neural network model believed to have an acceptable reliability.

As the existence of a difficulty to obtain more onsite survey data for the similar road section from other reports, the present study used a limited number of survey data for developing the neural network model, which might not be sufficient for predicting newly found slope failure cases. However, the total onsite survey data employed in this study provide a minimum sense of 30 data samples from statistical point of view. In addition, the neural network approach might converge to a local minimum during the calculation process, and that might have an influence on predicting accuracy. Instead of using different algorithms such as Fletcher-Powell Conjugate Gradient (CGF), Quasi-Newton (BFG), and Levenberg-Marquardt (LM), to see if there is any improvement in the results. The consideration of incorporating a genetic algorithm with a global searching capability in the neural network model, might well be a more suitable approach for future studies in this type of slope failure problem.

## ACKNOWLEDGMENT

The authors gratefully acknowledge the Central Weather Bureau of Taiwan for providing the recorded rainfall data. The English editing work throughout the paper by Mr. Michael A. Wise is also greatly appreciated.

## REFERENCES

- [1] Wikipedia, "Flooding disaster on 8th of August," Wikimedia Foundation, 2015, Available: <https://zh.wikipedia.org/wiki/%E5%85%AB%E5%85%AB%E6%B0%B4%E7%81%BD>.
- [2] Wikipedia, "Typhoon Morakot," Wikimedia Foundation, 2015, Available: [https://en.wikipedia.org/wiki/Typhoon\\_Morakot](https://en.wikipedia.org/wiki/Typhoon_Morakot).
- [3] R.N. Chowdhury, *Slope analysis, Developments in geotechnical engineering*, vol. 22, 1978, pp. 1-423, Elsevier Scientific Publishing Company.
- [4] E. Hoek, and J.D. Bray, *Rock slope engineering*, 1981, pp. 1-368, CRC Press.
- [5] C.G. Tung, C.N. Liu, and W.F., Lee, "Typhoon induced roadside slope failure and landslide mechanism along Alishan mountain road," *Geotechnique*, vol. 122, 2009, pp. 31-40.
- [6] S.C. Chang, *Feasibility assessment and investigation analysis of engineering topography and geology for facilities engineering of Tatung and Talee access road in the Taroko National Park*, Administration of Taroko National Park, 2004, pp. 98-98.
- [7] J.M. Abbas, "Slope stability analysis using numerical method," *Journal of Applied Sciences*, vol. 14, 2014, pp. 846-859.
- [8] K. Farah, M. Ltifi, and H. Hassis, "A probabilistic non-linear finite element analysis for slope stability problem," *the IES*

- Journal Part A: Civil & Structural Engineering*, 8(3), 2015, pp. 211-218.
- [9] R.H. Sharma, "Evaluating the effect of slope curvature on slope stability by a numerical analysis," *Austrian Journal of Earth Sciences*, vol. 60, 2013, pp. 283-290.
  - [10] J. Shen, and M. Karakus, "Three-dimensional numerical analysis for rock slope stability using shear strength reduction method," *Canadian Geotechnical Journal*, vol. 51, 2014, pp. 164-172.
  - [11] N. Li, and Y.M. Cheng, "Laboratory and 3-D distinct element analysis of the failure mechanism of a slope under external surcharge," *Natural Hazards and Earth System Sciences*, vol. 15, 2015, pp. 35-43.
  - [12] W. Shao, T.A. Bogaard, M. Bakker, and R. Greco, "Quantification of the influence of preferential flow on slope stability using a numerical modelling approach," *Hydrology and Earth System Sciences*, vol. 19, 2015, pp. 2197-2212.
  - [13] L. Ngai, Y. Wong, and Z. Wu, "Application of the numerical manifold method to model progressive failure in rock slopes," *Engineering Fracture Mechanics*, vol. 119, 2014, pp. 1-20.
  - [14] S. Nelson, *Slope stability, triggering events, mass movement hazards*, Natural Disasters, EENS 3050, 2013, pp. 1-17, Available: [http://www.tulane.edu/~sanelson/Natural\\_Disasters/slopestability.htm](http://www.tulane.edu/~sanelson/Natural_Disasters/slopestability.htm).
  - [15] H.J. Hwang, *Study on the potential landslide distribution and landuse conflict in Tchi reservoir watershed*, Master Thesis, NPUST, 2006, Taiwan.
  - [16] H. Chen, Z. Zeng, and H. Tang, "Landslide deformation prediction based on recurrent neural network," *Neural Processing Letters*, 41(2), 2015, pp. 169-178.
  - [17] Y. Erzsin, and T. Cetin, "The prediction of the critical factor of safety of homogeneous finite slopes using neural networks and multiple regressions," *Computers & Geosciences*, vol. 51, 2013, pp. 305-313.
  - [18] H.M. Lin, S.K., Chang, J.H. Wu, and C.H. Juang, "Neural network-based model for assessing failure potential of highway slopes in the Alishan, Taiwan area: pre- and post-earthquake investigation," *Engineering Geology*, 104(3-4), 2009, pp. 280-289.
  - [19] S.H. Ni, P.C. Lu, and C.H. Juang, "A fuzzy neural network approach to evaluation of slope failure potential," *Computer-Aided Civil and Infrastructure Engineering*, 11(1), 2008, pp. 59-66.
  - [20] B. Pradhana, and S. Lee, "Landslide susceptibility assessment and factor effect analysis: backpropagation artificial neural networks and their comparison with frequency ratio and bivariate logistic regression modelling", *Environmental Modelling & Software*, vol. 25, 2010, 747-759.
  - [21] I. Yilmaz, "Landslide susceptibility mapping using frequency ratio, logistic regression, artificial neural networks and their comparison: A case study from Kat landslides (Tokat-Turkey)," *Computers & Geosciences*, 35(6), 2009, pp. 1125-1138.
  - [22] Annual Report, *Disaster potential map*, National Science and Technology Center for Disaster Reduction, 2013, Available: <http://satis.ncdr.nat.gov.tw/Dmap/102news.aspx>.
  - [23] Water Resources Agency, *Hydrological year book of Taiwan ROC, part i - rainfall*, Ministry of Economic Affairs, 2007, Taiwan.
  - [24] K. Arai, "Visualization of learning processes for back propagation neural network clustering," *International Journal of Advanced Computer Science and Applications*, 4(2), 2013, pp. 234-238.
  - [25] H. Azami, M.R. Mosavi, and S. Sanei, "Classification of GPS satellites using improved back propagation training algorithms," *Wireless Personal Communications*, 71(2), 2013, pp. 789-803.
  - [26] G. Gandhimathi, C. Narmadha, and D. Kumar, "Simulation of narrow band speech signal using back-propagation neural networks," *International Journal of Computer, Mathematical Sciences and Applications*, 5(1-2), 2011, pp. 29-34.
  - [27] C.C. Gowda, and S.G. Mayya, "Comparison of back propagation neural network and genetic algorithm neural network for stream flow prediction," *Journal of Computational Environmental Sciences*, 2014, Available: <http://dx.doi.org/10.1155/2014/290127>.
  - [28] S. Solanki, and H.B. Jethva, "Modified back propagation algorithm of feed forward networks," *International Journal of Innovative Technology and Exploring Engineering*, 2(6), 2013, pp. 131-134.
  - [29] Y.C. Yeh, *Application of neural network*, Rulin Book Company, 2004, Taiwan.
  - [30] M. Moreira, and E. Fiesler, *Neural networks with adaptive learning rate and momentum terms*, IDIAP Technical Report, 95-04, 1995, pp. 1-30.
  - [31] R.A. Jacobs, "Increased rates of convergence through learning rate adaptation," *Neural Networks*, vol. 1, 1998, pp. 295-307.
  - [32] D. Demuth, and M. Beale, *Neural network toolbox user guide*, online, 2002, the Math works, Inc., USA.
  - [33] T. Kerh, Y.H. Su, and A. Mosallam, A., "Incorporating global search capability of a genetic algorithm into neural computing to model seismic records and soil test data," *Neural Computing & Applications*, online DOI 10.1007/s00521-015-2077-7, 2015, pp. 1-12.
  - [34] T. Kerh, D. Gunaratnam, and Y. Chan, "Neural computing with genetic algorithm in evaluating potentially hazardous metropolitan area result from earthquake," *Neural Computing & Applications*, 19(4), 2010, pp. 521-529.
  - [35] C.W. Dawson, and R.L. Wilby, Hydrological modelling using artificial neural networks. *Progress in Physical Geography*, 25(1), 2001, pp. 80-108.

## AUTHOR'S PROFILE



**Tienfuan Kerh** received his Ph.D degree from University of Southern California, in the United States. Currently, he is a full professor in civil engineering department, National Pingtung University of Science and Technology, Taiwan. He ever served as a visiting scholar in University of Sydney, Australia; University of London (University College London & Imperial College London), U.K.; University of Heidelberg, Germany; and University of California, Irvine, USA. His scientific interests include artificial intelligence applications in seismic data analysis, coastal line variation, and water resources. He also works in the field of computational fluid dynamics, emphasized in fluid-structure interaction. In addition to publish numerous journal and conference papers, he serves as an editorial member for several international journals and conferences. He also served as a reviewer for more than 20 international journals as listed in Science Citation Index.